Intranasal oxytocin administration rescues neonatal thermo-sensory deficit in mouse model of Autism

Laura Caccialupi Da Prato[1], Dina Abdallah[1], Vanessa Point[2], Fabienne Schaller[1], Emilie Pallesi-Pocachard[1], Aurélie Montheil[1], Stéphane Canaan[2], Jean-Luc Gaiarsa[1], Françoise Muscatelli[1], Valéry Matarazzo[1*]

[1] Aix Marseille Univ, INSERM, INMED, Marseille, France

[2] Aix-Marseille Univ, CNRS, LISM, IMM, Marseille, France

*: corresponding author

Email: valery.matarazzo@inserm.fr;

Institut de Neurobiologie de la Méditerranée (INMED)

INSERM-Aix Marseille Université, UMR1249

Campus Scientifique de Luminy, 13273 Marseille, France

Running short title: neonatal thermosensory reactivity in ASD

Keywords: thermo-sensory; Autism; Schaaf-Yang syndrome, Prader-Willi syndrome; Oxytocin

ABSTRACT

Atypical responses to sensory stimuli are considered as a core aspect and early life marker of autism spectrum disorders (ASD). Although recent findings performed in mouse ASD genetic models report sensory deficits, these were explored exclusively during juvenile or adult period. Whether sensory dysfunctions might be present at the early life stage and rescued by therapeutic strategy are fairly uninvestigated. Here we identified that neonatal mice lacking the autism-associated gene *Magel2* fail to react to cool sensory stimuli, while autonomic thermoregulatory function is active. This neonatal deficit was mimicked in control neonates by chemogenetic inactivation of oxytocin neurons. Importantly, intranasal administration of oxytocin was able to rescue the phenotype and brain Erk signaling impairment in mutants. This preclinical study establishes for the first-time early life impairments in thermosensory integration and shows the therapeutic potential benefits of intranasal oxytocin treatment on neonatal atypical sensory reactivity.

38 **INTRODUCTION**

39 Autism spectrum disorder (ASD) is a developmental disorder characterized by challenges with
40 social interaction, speech and non-verbal communication, as well as repetitive behaviors.
41 However, atypical sensory behaviors are a core aspect of ASD affecting 90% of children (*1*).
42 Importantly, sensory sensitivities have been documented as early as 6 months in ASD infants,
43 preceding considerably the common core features and the diagnosis (*2, 3*). Much of research
44 in animal models of syndromic and non-syndromic forms of ASDs has focused on the social
45 and cognitive difficulties and their underlying mechanisms (*1*). Recent increasing evidences
46 suggest that sensory traits such as tactile, visual, auditory, olfactory, gustatory and heat
47 abnormalities (*4-10*) are present in juvenile/adult ASD models (*11*). However, nor the
48 demonstration of sensory dysfunctions during early post-natal development nor the underlying
49 mechanism have been investigated. These are important steps for early diagnoses and
50 development of therapeutic strategies for ASD.

51 During the first week of life, sensory integrity is instrumental since neonates have to undertake
52 vital innate behaviors such as nipple-searching and alert calls. Among the various stimuli
53 arising from the external world, sensing any reduction of the ambient temperature is particularly
54 relevant for neonatal pups. Indeed, unlike their homeothermic adult counterparts, neonates
55 are poikilothermic (*12*) and should be kept in close contact with the mother in order to keep
56 their body temperature. In the absence of their warmth-giving mother and being exposed to
57 cool temperatures, neonates generate ultrasonic vocalizations (USV). In fact, during the
58 perinatal period, exposure to low ambient temperatures is considered as a major stimulus for
59 eliciting USV (*13-15*).

60 The neuronal pathways underlying cool response behavior is still under intensive investigation.
61 At the peripherical level, thermosensory neurons have been described in the skin and also in
62 the Grueneberg ganglion – a cluster of sensory neurons localized at the tip of the nose (*16-*
63 *19*). It has been proposed that this ganglion influences USV (*20*) generated by rodent neonates

to elicit maternal care on exposure to cool temperatures (*14, 15, 21*). Interestingly, neonate mice deleted for the thermoreceptor expressed in these sensory neurons present USV calls impairment after cool exposure (*17*). Following cool exposure, newborns require an effective thermoregulatory adaptative response to produce heat (*22*). During this period, the primary source of heat is produced by the sympathetically mediated metabolism of brown adipose tissue (BAT); also, so called non-shivering thermogenesis (*23*).

Here, using behavioral tests to assess neonatal thermosensory reactivity we discovered the existence of early developmental deficits in thermal sensitivity in neonate mice lacking the autism-associated gene *Magel2*. *MAGEL2* is an imprinted gene highly expressed in the hypothalamus that is paternally expressed and which paternal deletion and mutation cause Prader-Willi (*24*) and Schaaf-Yang (*25*); two syndromes with high prevalence of ASD (27% and 78% respectively). Both syndromes share overlap phenotype including feeding difficulties and hypotonia at birth followed by alterations in social behavior and deficits in cognition over lifespan. The patients have also sensory disorders characterized, in particular, by instability of body temperature manifested by episodes of hyper or hypothermia without infectious causes and which can be fatal in infants (*26, 27*). Moreover, adolescent with ASD present loss of sensory function for thermal perception (*28*).

With the aim to explore the physio-pathophysiological mechanism underlying this thermal deficit we explored peripheral functional activities of both Grueneberg ganglion and BAT. Furthermore, since this oxytocinergic system is considered as a rheostat of adult sensory functions (*29*), a modulator of huddling and thermotaxis behavior in response to cold challenge (*30*) and it is altered in *Magel2*$^{+/-p}$ neonate mice (*31, 32*), we investigated whether central dysfunction of the oxytocinergic system could sustain neonatal thermosensory reactivities and whether OT pharmacological treatment with OT agonists could be a therapeutical approach.

90

91

92 **RESULTS**

93 ***ASD-related Magel2 mutation leads to neonatal thermosensory behavior alterations***
94 ***during the first week of life***

95 To assess thermosensitivity in neonates, we developed an experimental procedure based on
96 coolness-induced USV (*17*) (Figure 1A). Wild-type (WT) and *Magel2*$^{+/-p}$ neonates aged from 0
97 to 6 days old (P0 to P6) were taken from their nests, isolated from the dam, and exposed
98 separately and successively to two different temperatures (ambient: 25°C and cool: 17°C). On
99 analyzing the latency in emitting the first call, which reflects the reactivity of the animals to
100 sense cold, we found that WT neonates presented a latency lower at cool temperatures than
101 under ambient exposure (Figure 1B-E-H-K), while *Magel2*$^{+/-p}$ did not (Figure 1C-F-I-L).
102 Furthermore, the responsive rate to cool temperature (i.e. the proportion of neonates
103 responsive to cooling) was markedly decreased in *Magel2*$^{+/-p}$ from P1 to P6 compared to the
104 WT (Figure 1D-G-J-M). Comparison of the latencies (Figure 1N-O) between WT and *Magel2*$^{+/-}$
105 ^{p} revealed a significant age-dependent difference under cool but not ambient exposure. This
106 deficit in sensory reactivity was independent of the sex. We also found that dam separation
107 and handling of *Magel2*$^{+/-p}$ did not affect corticosterone levels differently from WT and cannot
108 be linked to this atypical thermosensory reactivity (Supplemental Figure 1).
109 Furthermore, in order to exclude any potentiation of dam separation we run assays in which
110 USV box temperature was kept at 25°C during the two periods of USV recording (Figure 2A).
111 Using new cohorts of animals, we found that WT performed comparably upon repetitive
112 ambient temperature exposures (Figure 2B-C, and G-H). Moreover, we run experimental
113 paradigm inversion in which another cohort of animals was first exposed to 17°C and then to
114 25°C (Figure 2D). WT neonates still presented a low-latency response when exposed first to
115 cool *versus* ambient temperatures (Figure 2D, E-F, and G- H). Thus, latency of the first call of

116 isolated neonates was dependent on external temperature. As previously observed, we
117 confirmed that USVs responses to a cool challenge decreased as the pups matured (*33*). At
118 P6, only half of the WT animals were reactive upon cool exposure (Figure 1M). At P8, USV
119 responses were clearly produced independently of the exposed temperature (data not shown).
120 This responsiveness to cool stimuli is independent of mother separation and declines towards
121 adulthood, which is correlated with fur growth, opening of ear canals and the increasing
122 capability of rodents to develop other thermoregulatory capabilities such as seeking
123 comfortable temperature (*13-15, 34*).

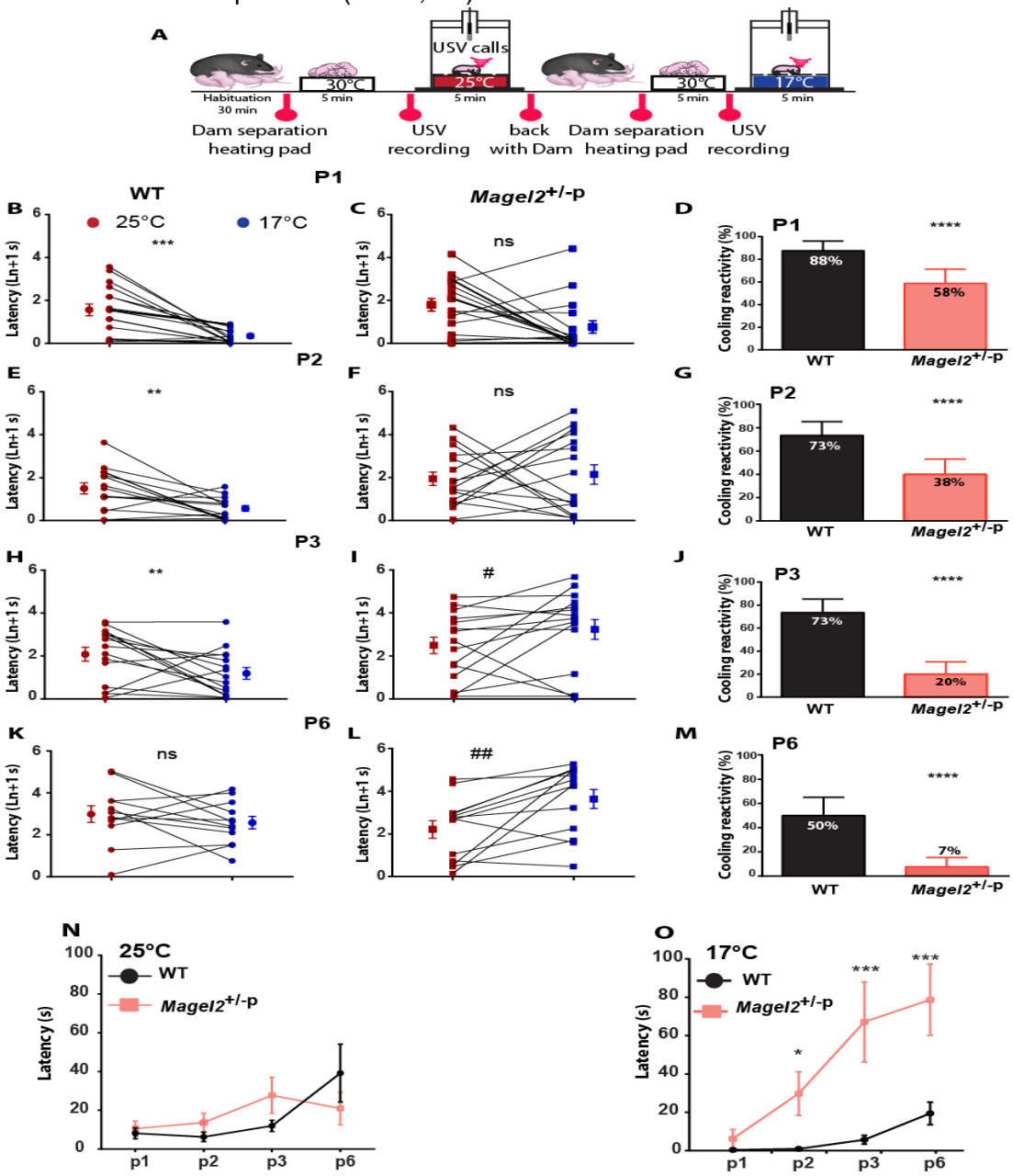

124 ***Figure 1. Coolness reactivity failure in Magel2 deficient neonates***

A *: Experimental procedure. After room habituation, neonates are separated from the dam, placed on a heating pad and each neonate is isolated for USVs recording at 25°C for 5 minutes. This procedure is repeated a second time at 17°C exposure and reconducted from P1 to P6 in WT and Magel2+/-p neonates.*

B-L*: Before/after graphs illustrating the latency to the first call measured upon exposure at 25°C (red dots) followed by 17°C (blue dots) in WT (B;E;H;K) and in Magel2+/-p (C;F;I;L). WT (25°C vs 17°C): P1: 1.56±0.27 ln+1 s vs 0.34±0.08 ln+1 s; n=16, p=0.0003; P2: 1.48±0.26 ln+1 s vs 0.55±0.13 ln+1 s; n=15, p=0.0054; P3: 2.08±0.32 ln+1 s vs 1.19±0.27 ln+1 s; n=15, p=0.0256; P6: 2.97±0.39 ln+1 s vs 2.56±0.29 ln+1 s, n=12, p=0.3804; Wilcoxon test. Magel2+/-p (25°C vs 17°C): P1: 1.79±0.29 ln+1 s vs 0.76±0.29 ln+1 s; n=17, p=0.0984; P2: 1.95±0.31 ln+1 s vs 2.14±0.45 ln+1 s; n=15, p=0.4037; P3: 2.5±0.38 ln+1 s vs 3.24±0.46 ln+1 s; n=16, p=0.0207; P6: 2.21±0.41 ln+1 s vs 3.65± 0.45 ln+1 s; n=13, p=0.0034; Wilcoxon test.*

D;G;J;M*: Bar graphs comparing animals responsive rate of coolness-stimulated USV between WT and Magel2+/-p neonates from P1 to P6. P1: WT: 87.5±8.5 %, n=16 vs Magel2+/-p: 58.82±12.3 %, n=17, p<0.0001; P2: WT: 73.33±11.82 %, n=15 vs Magel2+/-p: 37.5±12.5 %, n=16, p<0.0001; P3: WT: 73.33±11.82 %, n=15 vs Magel2+/-p: 20±10.69 %, n=15, p<0.0001; P6: WT: 50±15.08 %, n=12 vs Magel2+/-p: 7.69±7.69 %, n=13, p<0.0001; Fisher's exact test.*

N-O*: Comparison of the latencies to the first call over the age between WT and Magel2+/-p neonates at 25°C (N) and 17°C (O). Starting at P2, significant age-dependent differences under cool but not ambient exposure were observed: P2: WT 0.96±0.28 s, n=15 vs Magel2+/-p 29.81±11.32 s, n=15; p=0.03 ; P3: WT 5.71±2.26 s, n=15 vs Magel2+/-p 67.15±20.92 s, n=15, p=0.005; P6: WT 19.47±5.90 s, n=12 vs Magel2+/-p 78.69±18.59 n=12, p=0.007; two-way ANOVA, Bonferroni's post-test.*

*Data are presented as mean±SEM, *: p<0.05; **: p <0.01; ***: p<0.001; ****: p<0.0001; #: p<0.05; ##: p<0.01; ns: non-significant.*

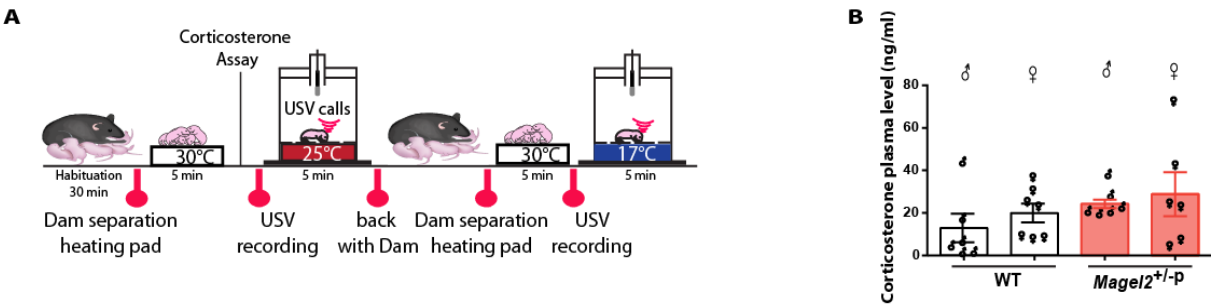

150

151 **Figure 1 supplemental 1.**

152 ***A****: Experimental procedure. After room habituation, neonates are separated from the dam, placed on a*

153 *heating pad for 5 minutes and blood samples are collected just before the USV recording.*

154 ***B****: Comparison between corticosterone plasma levels in female and male of WT and Magel2+/-p*

155 *measured when neonates are being isolated for USV calls. Males: WT: 12,974±6,711 ng/ml, n=6 vs*

156 *Magel2+/-p: 24,328±1,971 ng/ml, n=7, p=0.4740. Females: WT 19,983±4,425 ng/ml, n=7 vs Magel2+/-*

157 *p: 28,831±10,314 ng/ml, n=6, p=0.6723, two-way ANOVA, Bonferroni's post-test.*

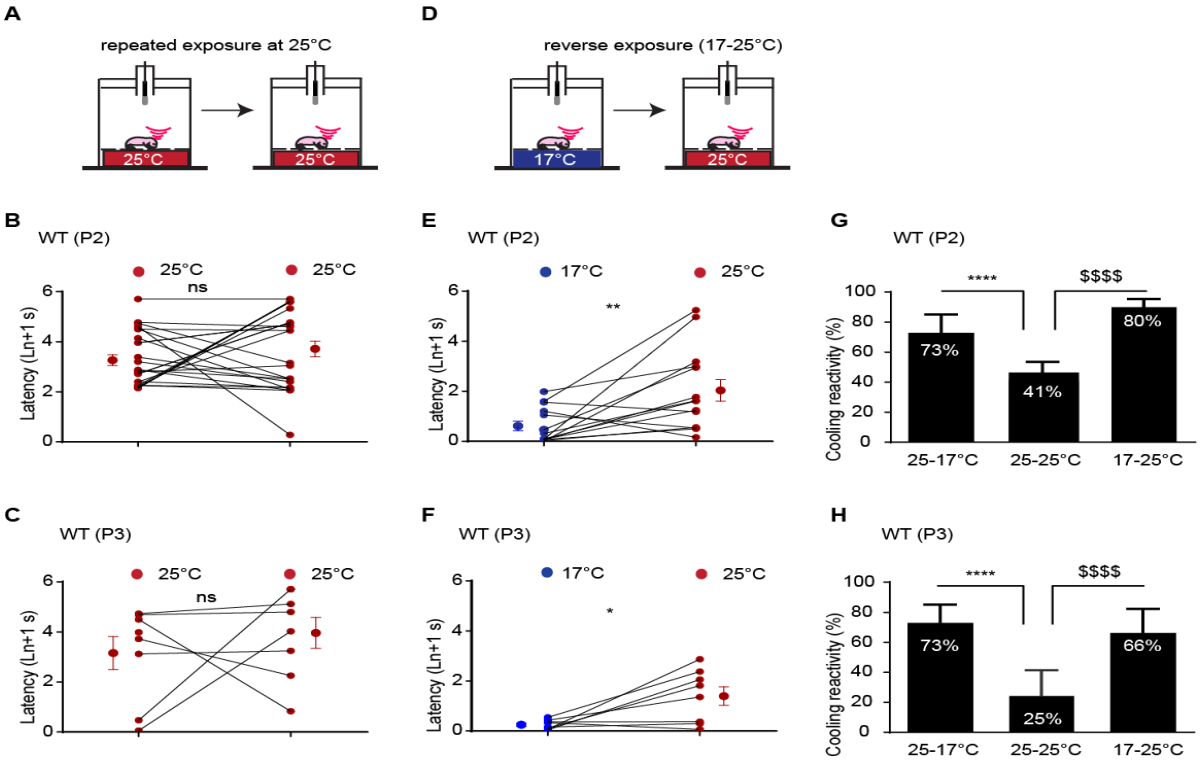

158 ***Figure 2. Coolness reactivity in WT upon repeated or reverse temperature exposures***

159 ***A-C**: Before/after graphs illustrating the latency to the first call measured upon a repeated exposure at*
160 *25°C (red dots) in WT at P2 (B) and P3 (C).*
161 ***D-F**: Before/after graphs illustrating the latency to the first call measured upon exposure at 17°C (blue*
162 *dots) followed by 25°C (red dots) in WT at P2 (E) and P3 (F). P2 WT (17°C vs 25°C) : 0.61±0.0.18 ln+1*
163 *s vs 2.03±0.43 ln+1 s; n=14, p=0.0.0052; P3 WT: 0.25±0.18 ln+1 s vs 1.40±1.05 ln+1 s; n=8, p=0.039;*
164 *Wilcoxon test.*
165 ***G-H**: Bar graphs showing WT animals responsive rate of coolness-stimulated USV at P2 (G) and P3*
166 *(H). P2 WT: 25°C-17°C: 73.33±11.82 %, n=15; 25°C-25°C: 41.18±12.30 %, n=17; 17°C-25°C:*
167 *85.71±9.70 %, n=14; *p<0.0001; $p<0.0001. P3 WT: 25°C-17°C: 73.33±11.82 %, n=15; 25°C-25°C:*
168 *25.00±16.37 %, n=8; 17°C-25°C: 66.67±16.67 %, n=9 ; *p<0.0001; $p<0.0001; Fisher's exact test. Data*
169 *are presented as mean±SEM **: p <0.01; ***: p<0.001; ns: non-significant.*
170

171 ***Cool thermo-sensory behavior impairment in Magel2$^{+/-p}$ neonates is not linked to a***
172 ***deficiency in non-shivering thermogenesis***

173 With the aim to uncover the physio-pathological mechanisms underlying this neonatal thermo-
174 sensory deficit, we first investigate for any thermogenesis dysregulation. Following cool
175 exposure, newborns require an effective thermoregulatory adaptative response to produce
176 heat (*22*). During this period, the primary source of heat is produced by the sympathetically
177 mediated metabolism of brown adipose tissue (BAT); also, so called non-shivering
178 thermogenesis (*23*). Activation of this cold-defensive response is dependent on a thermal
179 afferent neuronal signaling, which involved peripheral thermoreceptors, namely TRPM8,
180 located in dorsal root ganglia sensory neurons of the skin (*35*).
181 Magel2 being expressed in dorsal root ganglia (*36, 37*), we first analyzed whether peripheral
182 expression of TRPM8 could be affected in *Magel2*$^{+/-p}$ compared to WT neonates. We found no
183 significant difference of the TRPM8 transcript (Figure 3A).
184 We also found that *Magel2* is expressed in BAT (Figure 3B) and that P2 *Magel2*$^{+/-p}$ neonates
185 had significant decreased interscapular mass BAT compared to aged-matched WT (Figure

186 3C). As previously shown, we found that in WT the mass of BAT was developmentally down-
187 regulated in WT. Such mass BAT declining in WT was not observed in mutant (Figure 3C).

188 In order to verify whether this difference of BAT mass could impact non-shivering
189 thermogenesis activity, we investigated BAT function through the analyses of BAT lipolysis
190 and the mitochondrial expression of the uncoupling protein 1 (UCP1) (*38*). In order to observe
191 BAT activation, interscapular BAT tissues from P2 pups were extracted after 1-hour exposure
192 to cool temperature (17°C). Quantitative analyses of BAT lipids, separated by thin layer
193 chromatography (Figure 3D-G), show that although cold exposure induced a significant
194 consumption of triglycerides in both WT and Magel2+/-p pups (Figure 3H), levels of
195 diglycerides and FA remained surprisingly unchanged for both genotypes (Figure 3I-J). Our
196 observation that BAT FA are not consumed upon cold exposure are consistent with recent
197 findings controverting the current view that BAT-derived FA are essential for thermogenesis
198 during acute cold (39).
199

200 Next, we found that upon acute cool exposure (17°C, 1h), UCP1 protein expression, a
201 mitochondrial protein activity marker from BAT responsible for non-shivering thermogenesis
202 significantly increases in P2 WT (Figure 3K-L) as well as Magel2+/-p (Figure 3M-N). Similar
203 results were observed at the age of P6 (Figure 3O-P, Q-R). Thus, these results demonstrate
204 that UCP1-mediated non-shivering thermogenesis in BAT is fully active in Magel2 deficient
205 pups. They are also consistent with recent findings showing that UCP1 activation is
206 independent of BAT mass and BAT-derived FA (39). We finally followed skin body
207 temperatures upon cool temperature challenge and found that temperature of Magel2 deficient
208 neonates drop similarly as WT (Figure 3S).
209 Altogether, our results demonstrate that lack of cool thermosensory call behavior found in
210 Magel2 deficient neonates is not related to their capacity of regulating temperature.
211

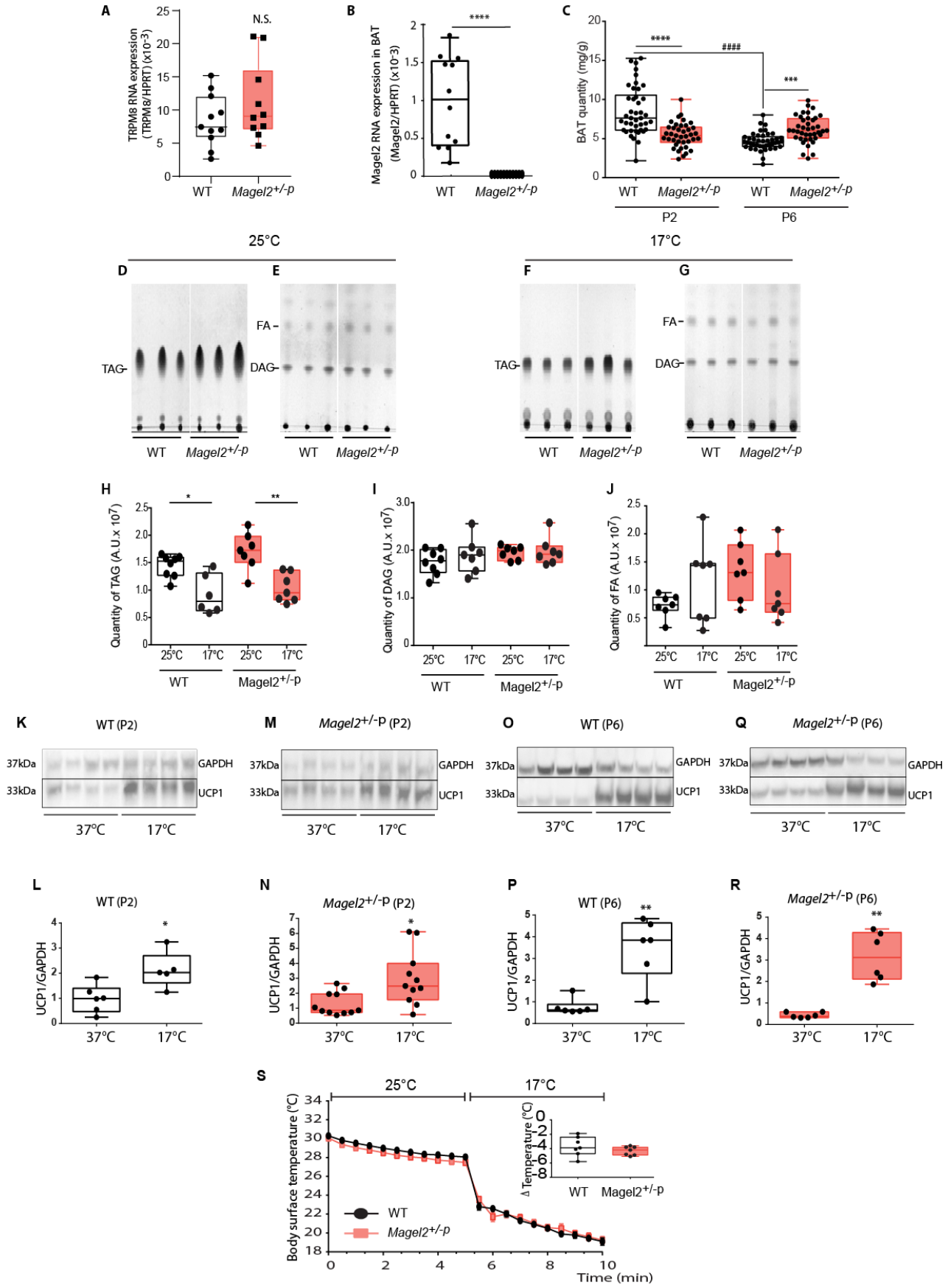
A
TRPM8 RNA expression (TRPM8/HPRT) (x10-3)
N.S.
WT
Magel2+/-p
B
Magel2 RNA expression in BAT (Magel2/HPRT) (x10-3)
****
WT
Magel2+/-p
C
BAT quantity (mg/g)
****
####
***
WT
Magel2+/-p
WT
Magel2+/-p
P2
P6
25°C
17°C
D
E
F
G
TAG
FA
DAG
WT
Magel2+/-p
H
Quantity of TAG (A.U.x 10^7)
25°C
17°C
25°C
17°C
WT
Magel2+/-p
I
Quantity of DAG (A.U.x 10^7)
J
Quantity of FA (A.U.x 10^7)
K
WT (P2)
M
Magel2+/-p (P2)
O
WT (P6)
Q
Magel2+/-p (P6)
37kDa
33kDa
GAPDH
UCP1
37°C
17°C
L
WT (P2)
N
Magel2+/-p (P2)
P
WT (P6)
R
Magel2+/-p (P6)
UCP1/GAPDH
S
25°C
17°C
Body surface temperature (°C)
Δ Temperature (°C)
WT
Magel2+/-p
Time (min)

212

213 ***Figure 3. TRPM8 and brown adipose tissue investigations after cool exposure in***
214 ***WT and Magel2+/-p***

215 ***A****: mRNA expression of TRPM8 in dorsal root ganglia. Quantification of TRPM8 RNA transcripts in*
216 *Dorsal root ganglia of WT and Magel2+/-p at P2. WT: 0.007 (0.005; 0.012), n=11 vs Magel2+/-p: 0.009*
217 *(0.007, 0.016), n=10, p=0.34, Mann Whitney test. Data are presented as median (with interquartile*
218 *range) (n=10).* ***B****: Quantification of Magel2 RNA transcripts in WT and Magel2+/-p in BAT and*
219 *hypothalamus at P2. WT BAT: 1.03x10-3(4.20x10-4; 1.53x10-3), n=12; WT hypothalamus: 3.79x10-2*
220 *(3.14x10-2; 4.53x10-2), n=24, *p=0.0006; $p<0.0001; Kruskal-Wallis test, Dunn's post-test.* ***C****: Brown*
221 *adipose tissue (BAT) weight normalized to the body weight of WT and Magel2+/-p at P2 and P6. P2:*
222 *WT 8.52±0.47 mg/g, n=42 vs Magel2+/-p: 5.25±0.26 mg/g, n=40, p<0.0001; P6: WT: 4.66±0.17 mg/g,*
223 *n=42 vs Magel2+/-p: 6.18±0.27 mg/g, n=40, p=0.0045, two-way ANOVA, Bonferroni's post-test; (**
224 *between genotype; # intragenotype).* ***D-J****: Total lipid extraction of WT and Magel2+/-p BAT and thin*
225 *layer chromatography analysis of TAG, DAG and FA.* ***H-J****: Quantifications of TAG (H), DAG (I) and FA*
226 *(J).* ***K-R****: Immunoblot analyses and quantifications of UCP1 expression after cool exposure at P2 (K-N)*
227 *in WT and Magel2+/-p (respectively K-L and M-N) and at P6 (O-R) in WT and Magel2+/-p (respectively*
228 *O -P and Q-R). L: WT P2 :0.99 (0.48, 1.41), n=6, vs 2.03 (1.61, 3.25), n=5, p=0.0173; N: Magel2+/-p*
229 *P2: 0.86 (0.71, 1.95), n=11, vs 2.49 (1.56, 4), n=11, p=0.0104. P: WT P6: 0.62 (0.57; 0.89), n=6, vs 3.84*
230 *(2.31; 4.64), n=6, p=0.0043; R: Magel2+/-p P6: 0.38 (0.32; 0.58), n=6, vs 3.12 (2.11; 4.29), n=6,*
231 *p=0.0022.* ***S****: Time course of loss of surface body skin temperature in WT (black line) and Magel2+/-p*
232 *(red line) of P2 neonates during a temperature challenge (5 minutes at 25°C then 5 minutes at 17°C).*
233 *Data are presented as mean±SEM. Insert represents the delta loss of surface body temperature before*
234 *(at 5 min) and after cool exposure (at 10 min) in WT and Magel2+/-p P2 neonates. WT: -3.9 (-4.7; -2.4),*
235 *n=7 vs Magel2+/-p -4.2 (-4.9;-3.8), n=7, p=0.3648; Mann Whitney test. Mann Whitney test. Data are*
236 *presented as median (with interquartile range), *: p<0.05; **: p<0.01.*

237

238 ***Cool thermo-sensory behavior impairment in Magel2$^{+/-p}$ neonates is not linked to***
239 ***dysfunction of the peripheral thermosensitive neurons from the Grueneberg ganglion***

240 Peripheral perception to cool temperature is also conducted by the Grueneberg ganglion, a
241 sensory organ located at the tip of the nose (figure 4 A). This ganglion contains sensitive

242 neurons responding to cool temperatures (*18*) and it has been proposed to influence USV (*20*)
243 generated by rodent neonates to elicit maternal care on exposure to cool temperatures (*14,*
244 *15, 21*). Interestingly, neonate mice deleted for the thermoreceptor expressed in these sensory
245 neurons present USV calls impairment after cool exposure; a phenotype very similar to what
246 we observe here in *Magel2*$^{+/-p}$ (*17*). We thus ask whether dysfunction of these peripheral
247 thermos-sensory neurons might be affected in *Magel2*$^{+/-p}$. We conducted calcium 2-photon
248 imaging on tissue slices through the Grueneberg ganglion of P2 neonates (Figure 4B-C).
249 Thermo-evoked neuronal activities (obtained by decreasing the temperature of the perfusion
250 solution from 35°C to 17°C) elicited a substantial increase in intracellular Ca^{2+} in both all WT
251 and *Magel2*$^{+/-p}$ animals tested (Figure 4D-E). Thus, the thermosensory neurons of the
252 Grueneberg ganglion are functional in the *Magel2*$^{+/-p}$ neonates.

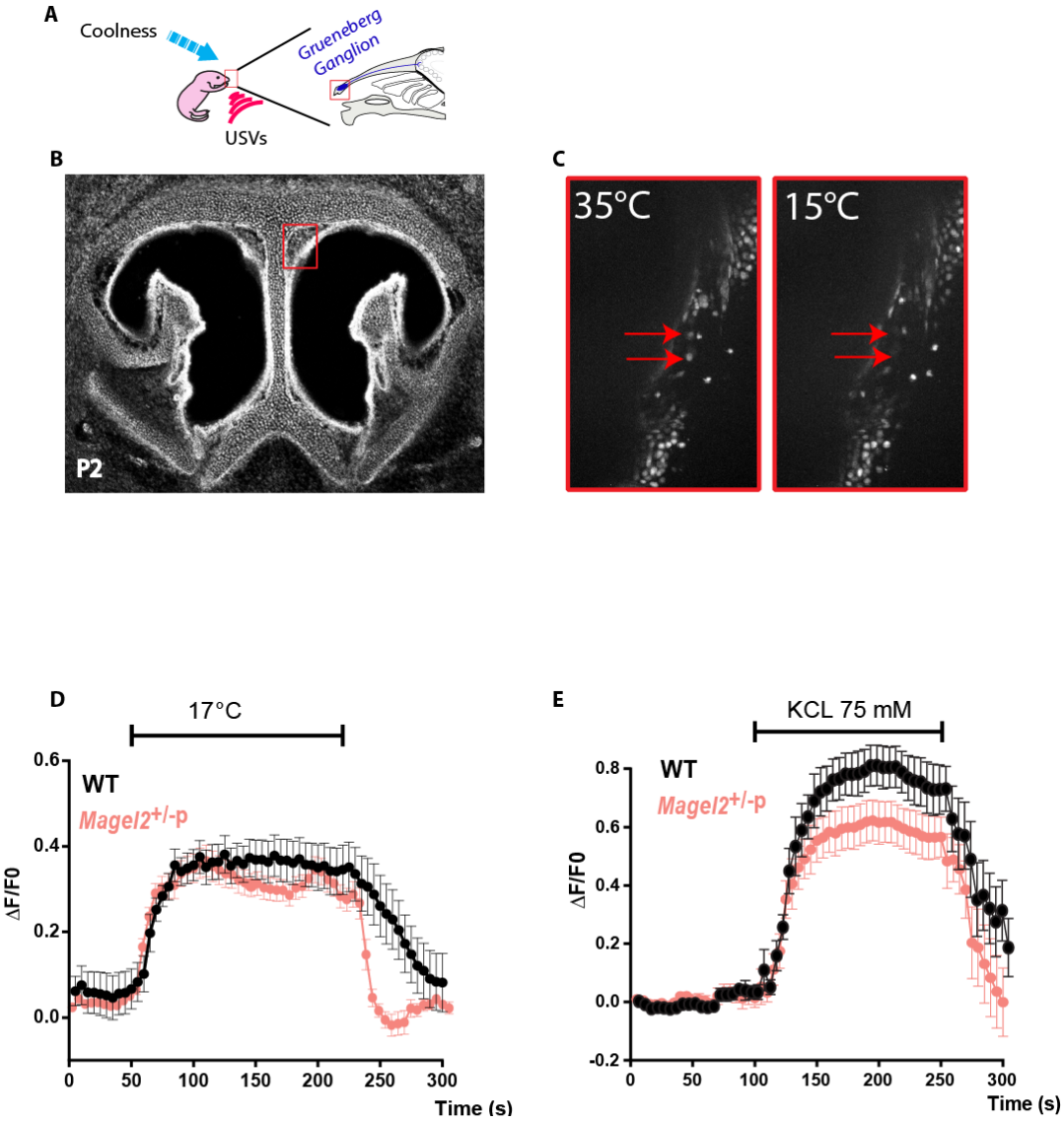

255 ***Figure 4. Coolness induced response in the Grueneberg Ganglion (GG) of Magel2+/-p.***

256 ***A****: Schematic representation of the role and localization of the GG.* ***B*** *: Coronal sections of the nasal*
257 *cavity of a P2 neonate with localization of the GG (red box).* ***C****: Inserts represent calcium imaging*
258 *responses after cool exposure.* ***D****: Representative Ca2+ signals induced by cooling from 35°C to 15°C*
259 *in WT (n=8) and Magel2+/- p (n=9) GG neurons (respectively black and red).* ***E****: Representative Ca2+*
260 *signals induced in GG neurons by perfusion with KCl (75 mM) were used as a control for viability and*
261 *responsiveness of tissues slices in WT (n=10) and Magel2+/-p (n=11) GG neurons. ΔF represents*
262 *change in the ratio of the fluorescence intensity; Data are represented as Mean±SEM.*

263

264 ***Neonatal inactivation of hypothalamic oxytocinergic neurons in WT mimics cool***
265 ***thermo-sensory behavior impairment found in Magel2$^{+/-p}$***

266 Oxytocin (OT) is a main neuropeptide involved in mediating the regulation of adaptive
267 interactions between an individual and his environment (*39*), in major part by modulating
268 sensory systems (*29*). To directly address the involvement of OT neurons in neonatal
269 thermosensory reactivity, we assessed whether inactivation of OT neurons of WT
270 hypothalamus neonates can mimic thermosensory impairment observed in *Magel2*$^{+/-p}$ using
271 DREADD (Designer Receptors Exclusively Activated by Designer Drugs) technology (*40*).
272 This DREADD receptor can be activated by the ligand clozapine N-oxide (CNO) and its
273 metabolite, clozapine; both drugs crossing the BBB (*41*). We restricted hM4Di-mCherry
274 expression to OT neurons by crossing hM4Di-mCherry mice (named here hM4Di) with OT Cre
275 mice in order to drive the expression of the receptor with the OT promoter (Figure 5A-B). These
276 mice were called here OThM4Di.

277 Vehicle or CNO (1µg) was injected into P2 neonates by intraperitoneal (IP) administration two
278 hours before starting thermo-sensory behaviors (Figure 5C). We found that vehicle-treated
279 DREADDs-expressing animals, OThM4Di, presented a significant faster reaction in emitting
280 their first call when exposed to cool *versus* ambient temperatures (Figure 5D); while CNO-
281 treated OThM4Di did not (Figure 5E). Furthermore, the animal responsive rate to cool
282 temperature was markedly decreased in CNO-treated OThM4Di with percentages reaching

similar values than *Magel2*$^{+/-p}$ neonates (Figure 5F). CNO treatment did not affect the numbers of USV calls of OThM4Di neonates either at ambient (25°C) or cool temperature (17°C); the number of USV calls being similar to *Magel2*$^{+/-p}$ neonates (Figure 5G-H).

To test for any possible side effects of CNO that were not DREADDs mediated, CNO was administered either to non-DREADDs-expressing (hM4Di) or WT P2 neonates. We found that the responsive rate to cool temperature was damped after CNO administration in WT and in CNO-treated hM4Di neonates (Figure 5F), while the number of USV calls remained similar either at ambient (25°C) or cool temperature (17°C) (Figure 5G and H). However, after CNO treatment responsive rate to cool temperature was still significantly lower in OThM4Di than in hM4Di neonates (Figure 5F). Thus, beside a side effect of CNO which has been reported in other behavioral tests (*42*), our results revealed that *in vivo* inactivation of OT neurons prevents neonates to respond to cool temperature and suggest that OT system can regulate cool sensitivity call behavior in neonates.

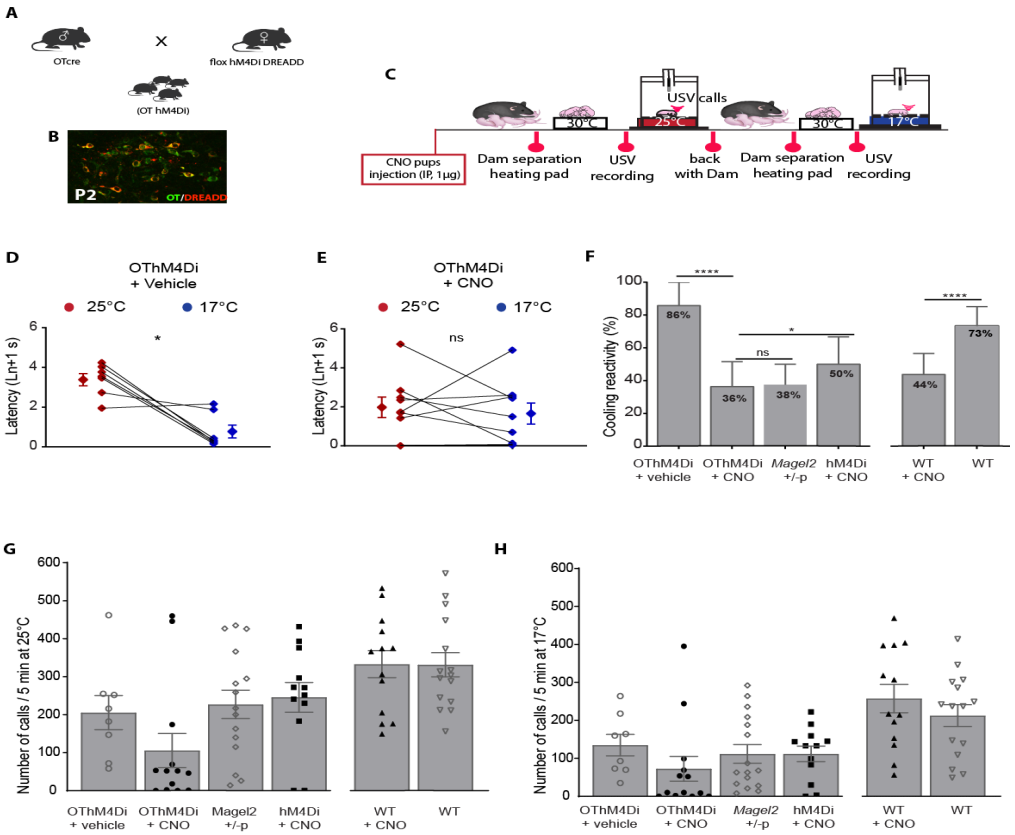

298

299 ***Figure 5. Coolness reactivity failure in WT after oxytocinergic neurons***
300 ***inactivation.***

301 ***A:*** *Generation of the hM4Di Dreadd OTCre mice (OThM4Di).* ***B****: Immunohistochemistry illustrating the*
302 *expression of hM3Di (red) in OT neurons (green).* ***C:*** *Experimental procedure: IP injection of CNO (1*
303 *µg) or vehicle was performed in P2 neonates 2 hours before starting experiment.* ***D-E****: Before/after*
304 *graphs illustrating the latency to the first call measured upon exposure at 25°C (red dots) followed by*
305 *17°C (blue dots) in neonates expressing the hM4Di receptor (OThM4Di) treated with vehicle (D):*
306 *3.39±0.3 ln+1 s vs 0.78±0.32 ln+1 s, n=7, p=0.0313 or treated with CNO (E): 1.97±0.52 s vs 1.65±0.54*
307 *ln+1 s, n=9, p=0.8203; Wilcoxon test.* ***F****: Responsive rate of coolness-stimulated USV in OThM4Di*
308 *neonates treated with vehicle or CNO (85.71±14.29 %, n=7 vs 36.36±15.21 %, n=11; p<0.0001). Cooling*
309 *reactivity of OT hM4Di neonates treated with CNO was also compared with either MageI2+/-p (37.5±12.5*
310 *%, n=16; p=0.1169) or neonates non-expressing the hM4Di receptor (hM4Di) (50±16.67 ln+1 s, n=10,*
311 *p=0.0315). The last bar graphs illustrate the effect of CNO treatment on WT neonates: WT: 73.33±11.82*
312 *%, n=15 vs WT+CNO: 43.75±12.81 %, n=16, p<0.0001; Fischer's exact test.* ***G-H****: Total number of calls*
313 *at 25°C (G) and 17°C (H) in OThM4Di neonates treated or not with CNO and compared with either*
314 *MageI2+/-p or neonates non-expressing the hM4Di receptor (hM4Di). The last two bar graphs illustrate*
315 *the effect of CNO treatment on WT neonates. Data are presented as mean±SEM *: p<0.05; **: p<0.01;*
316 ****: p<0.001; ****: p<0.0001.*

317

318 ***Intranasal injection of Oxytocin rescues cool sensitivity call behavior in MageI2+/-p***
319 ***neonates***

320 We ask whether pharmacological OT treatment could improve thermosensory call behavior in
321 the *MageI2*$^{+/-p}$ during neonatal period (P2). Of the two preferred routes to reach the
322 cerebrospinal fluid, and considering the small size of neonate mice, we found more convenient
323 to administrate OT by intranasal (IN) rather than intravenous route (*43, 44*). New cohorts of
324 neonatal mice were tested for cool thermosensory call behavior with a similar procedure except
325 that neonates received the treatment in between ambient and cool exposures. This procedure

326 allows us to analyze the effect of an acute OT treatment by comparing ambient *versus* cool
327 exposure responses within a same animal (Figure 6A).
328 We first verified that handling and IN administration procedures did not affect cool-induced call
329 behavior of *Magel2*$^{+/-p}$ neonates by comparing untreated and vehicle-treated groups. After
330 vehicle treatment (saline solution), *Magel2*$^{+/-p}$ were unable to react to cool exposure since the
331 latency to the first call under cool exposure was similar to ambient exposure (Figure 6B).
332 Furthermore, comparison of the responsive rate to cool temperature (i.e. the proportion of
333 neonates responsive to cooling) under cool exposure revealed insignificant change between
334 these control groups (Figure 6C).
335 We found that IN administration of OT (2 µg) significantly decreased the latency of the first call
336 of *Magel2*$^{+/-p}$ neonates under cool exposure (Figure 6D) and the responsive rate was markedly
337 increased in *Magel2*$^{+/-p}$ (Figure 6E). Indeed, after OT injection, 77% of *Magel2*$^{+/-p}$ neonates
338 reacted to cool stimuli, a percentage similar to the P2 WT (Figure 6L). Thus, an OT
339 pharmacological treatment is able to rescue the cool thermosensory call behavior deficit of the
340 *Magel2*$^{+/-p}$ neonates.
341 To better characterize the pathway implicated in the rescue of the cool-induced call behavior,
342 we tested OT agonists. OT and vasopressin (AVP) are closely related nonapeptides that share
343 high sequence and structure homology (*45*). Although one unique receptor exists for OT in
344 mammals, AVP can also bind and activate the OT receptor with the same affinity as OT (*46*).
345 Among the different agonist developed for the OT receptor, [Thr^{4},Gly^{7}]OT also referred to as
346 TGOT, has been widely used as a selective OT agonist (*46*); We thus treated *Magel2*$^{+/-p}$
347 neonates (P2) with either TGOT or AVP and performed USV call recording 10 min after
348 administration of the agonist dose. By analyzing the reactivity of the animals to sense cool
349 temperature, we found that *Magel2*$^{+/-p}$ neonates (P2) presented a significant faster reaction in
350 emitting their first call when exposed to cool *versus* ambient temperature after either TGOT or
351 AVP treatment (Figure 6F and H, respectively). Furthermore, the responsive rate of *Magel2*$^{+/-}$
352 ^{p} neonates to cool temperature was markedly increased in both TGOT and AVP conditions
353 (Figure 6G and I, respectively); reaching similar values as the P2 WT (Figure 6L). We also

354 addressed the action of TGOT in WT neonates and found that it still preserved both the
355 response and the number of USV upon cool temperature exposure (Figure 6J-L and N).
356 Finally, *Magel2*$^{+/-p}$ pups treated either with AVP or TGOT evoked substantial USV call number
357 upon cool exposure (Figure 6M), with values similar to P2 WT (Figure 6L). Although we cannot
358 completely exclude a minor contribution of the AVP receptors, these data suggest that the
359 rescue of cool thermosensory call behavior is mainly due to activation of the OT receptors.

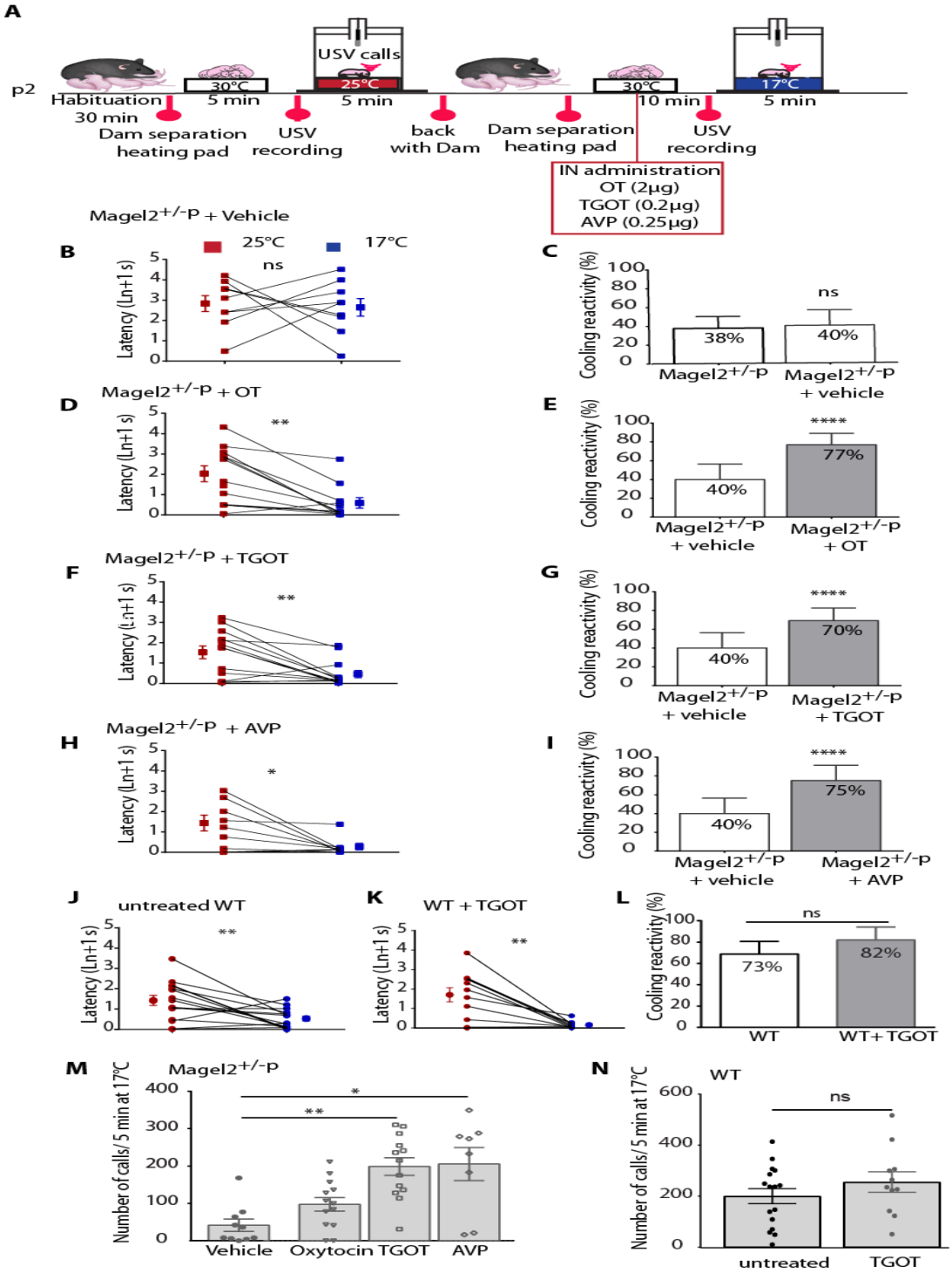

360 ***Figure 6. Intranasal oxytocin and oxytocin receptor agonists rescue coolness reactivity***
361 ***in Magel2+/-p.***

362 *A: Experimental procedure. After room habituation, Magel2+/-p neonates (P2) are separated from the*
363 *dam, placed on a heating pad and each neonate is isolated for USVs recording at 25°C for 5 min. 10*
364 *minutes before repeating the procedure at 17°C, neonates receive an intranasal injection (IN) of Vehicle*
365 *(NaCl), or Oxytocin (OT, 2 µg) or (Thr4,Gly7)-Oxytocin (TGOT, 0.2 µg) or Vasopressin (AVP, 0.25 µg).*
366 *B;D;F;H: Before/after graphs represent the latency to the first call measured at 25°C (red dots) and 17°C*
367 *(blue dots) in Magel2+/-p treated with vehicle (B: 2.83±0.39 ln+1 s vs 2.64±0.43 ln+1 s, n=9, p=0.9102),*
368 *OT (D: 2.03± 0.39 ln+1 s vs 0.59±0.25 ln+1 s, n=13, p=0.0049), TGOT (F: 1.54±0.31 ln+1 s vs 0.47±0.18*
369 *ln+1 s, n=13, p=0.0061) and AVP (H: 1.44±0.39 ln+1 s vs 0.28±0.16 ln+1 s, n=8, p=0.0156); Wilcoxon*
370 *test.*
371 *C;E;G;I: Bar graphs showing animals responsive rate of coolness-stimulated USV in Magel2+/-p*
372 *untreated or treated with vehicle (C: 37.5±12.5 % n=16 vs 40±16.33 %, n=9, p=0.7714), treated with*
373 *vehicle or OT (E: 40±16.33 %, n=9 vs 76.92±12.16 %, n=13, p<0,0001), or TGOT (G: 69.23±13.32 %,*
374 *n=13, p<0.0001) or AVP (I: 75±16.37 %, n=8, p<0.0001); Fisher's exact test.*
375 *J-K: Latency to the first call measured at 25°C (red dots) and 17°C (blue dots) in untreated (J: 1.48±0.26*
376 *ln+1 s vs 0.55±0.13 ln+1 s, n=15, p=0,0054) or TGOT-treated WT (K: 1.71± 0.37 ln+1 s vs 0.16± 0.05*
377 *ln+1 s, n=11, p=0.0049); Wilcoxon test.*
378 *L: Responsive rate of coolness stimulated USV in untreated WT compared with TGOT-treated WT*
379 *(73.33±11.82 % n=15 vs 81.82±12.20 %, n=11, p=0.2393).*
380 *M: Total number of calls recorded during 5 minutes in Magel2+/-p treated with vehicle (41.3±16.48,*
381 *n=10) and compared with OT (97.31±18.16%, n=13, p=0.45), or TGOT (198.50±23.45 %, n=13,*
382 *p=0.006), or AVP (205.30±44.03 %, n=10, p=0.0035); Kruskal-Wallis test, Dunn's post-test. N: Total*
383 *number of calls in untreated WT compared with TGOT-treated WT at 17°C (200.1±29.85, n=16 vs*
384 *255.5±39.92, n=11, p=0.5039); Mann Whitney test. Data are presented as mean±SEM, *: p<0.05; **:*
385 *p<0.01; ***: p<0.001; ****: p<0.0001.*
386
387
388
389

390 ***Oxytocin rescues Magel2$^{+/-p}$ brain Erk signaling impairment after cool stimuli***

391 Since cool exposure or stress alters the Erk pathways in the brain by reducing Erk activation
392 (*47, 48*) and OT has been shown to block this alteration (*47*), we examined whether this
393 signaling pathways might be altered in *Magel2*$^{+/-p}$ brain neonates. Erk/P-Erk levels were
394 measured from P2 whole brains of WT and *Magel2*$^{+/-p}$ immediately after ambient or cool
395 exposure. Cytoplasmic levels of P-Erk revealed that brain of WT neonates had a significant
396 cool-induced reduction of P-Erk (Figure 7A and C); while *Magel2*$^{+/-p}$ did not (Figure 7B and D).
397 More importantly, IN administration of OT allowed a cool-induced reduction of P-ErK in the
398 *Magel2*$^{+/-p}$ neonates (Figure 7F and H) without affecting the reduction of P-ErK in the brain of
399 WT (Figure 7E and G). Thus, these results highlight a deficit in *Magel2*$^{+/-p}$ brain development
400 and reveal that OT's ability to reverse cool thermosensory call behavior may act, at least partly,
401 through Erk pathway.

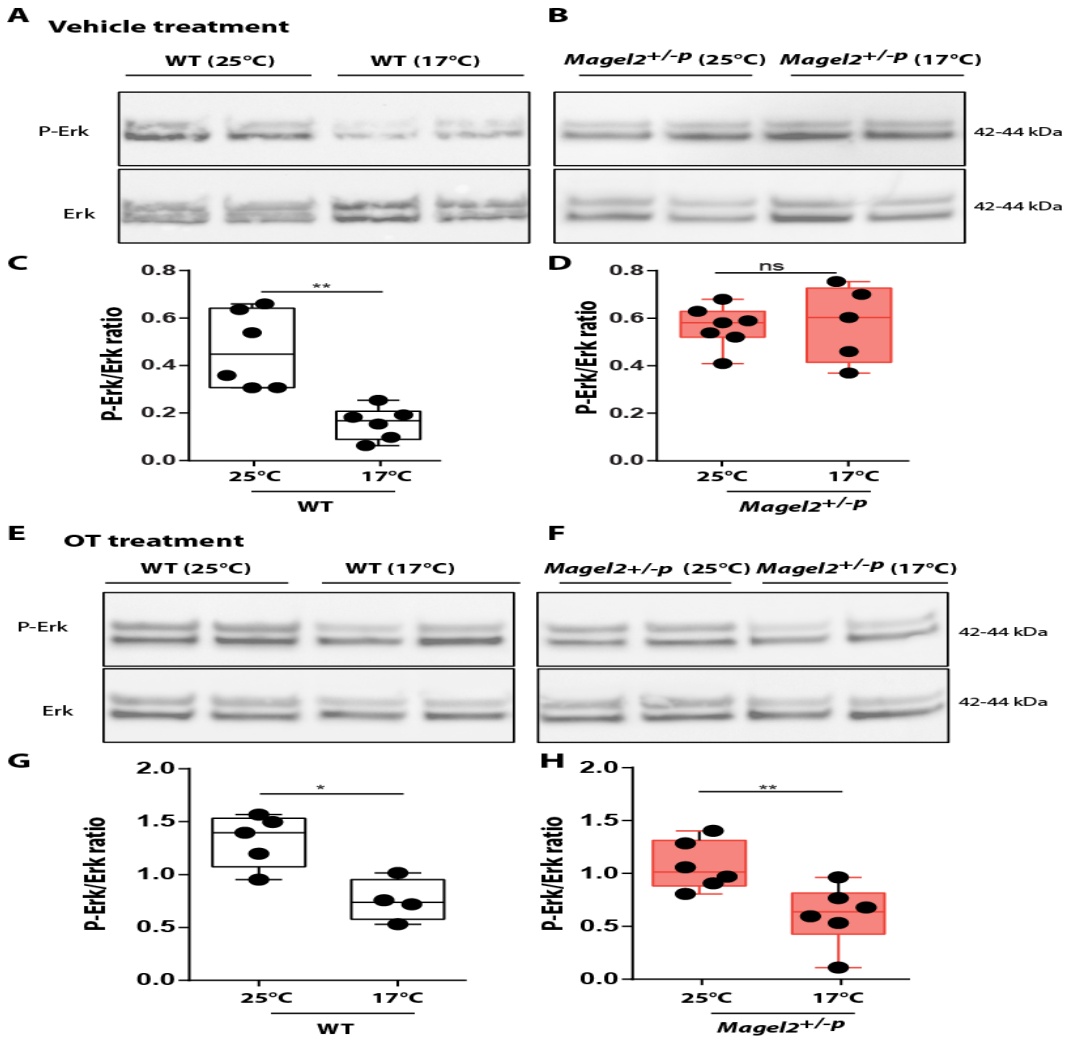

402 ***Figure 7. Extracellular signal-regulated kinase (ERK) signaling after cool exposure and***
403 ***oxytocin treatment***

404 *A-B: Representative Western blots of cerebral ERK and phosphorylated ERK (pERK) issued from*
405 *vehicle-treated WT (A) and Magel2+/-p (B) exposed to 25 or 17°C. C-D: Western-blots quantification*
406 *from WT (C): 0.47±0.07 vs 0.16±0.03, n=6, p=0.0022 or Magel2+/-p (D): 0.56±0.03, n=7 vs 0.58±0.07,*
407 *n=5, p=0.7424; Mann Whitney test.*

408 *E-F: Representative Western blots of cerebral ERK and phosphorylated ERK (pERK) issued from*
409 *intranasal OT-treated WT (E) and Magel2+/-p (F) exposed to 25 or 17°C. G-H: Corresponding western-*
410 *blots quantification from WT (G): 1.32±0.11, n=5 vs 0.76±0.1, n=4, p=0.0317 or Magel2+/-p (H):*
411 *1.08±0.09, n=6 vs 0.62±0.12, n=6, p=0.0087; Mann Whitney test. *: p<0.05; **: p<0.01; ns: non-*
412 *significant.*

413

414

415 **DISCUSSION**

416 ASD research has mainly focused on ASD-related genes and their impact on social and
417 cognitive behavior in adult. However, atypical sensory reactivity that represents early markers
418 of autism and are predictive of social-communication deficits and repetitive behaviors in
419 childhood has been largely overlooked. Although recent findings performed in mouse ASD
420 genetic models report sensory deficits (*4-10*), they were explored during juvenile or adult
421 period. Whether sensory dysfunctions might be present at the early life stage is still unknown.
422 Here we provide the first experimental evidence that newborn harboring deletion in *Magel2*, *a*
423 gene implicated in Prader-Willi and Shaaf-Yang, two syndromes presenting ASD phenotype,
424 exhibit atypical sensory behavior during the first postnatal week.
425 With the aim to investigate a relevant sensory function during early life, we explored the
426 thermosensory function. Indeed, sensing any reduction of the ambient temperature is
427 particularly vital, since neonates are poikilothermic. In contrast to adult who can adopt diverse

428 strategies in response to cool stimuli such as thermoregulatory behavior and shivering
429 thermogenesis, newborns need to stay with their warmth-giving mother. In absence of this
430 warming, cool exposure elicits an innate behavior characterized by USV emissions. Here we
431 found that deletion of *Magel2* leads to a hyporeactivity in emitting the first call when neonates
432 are isolated from their dam and exposed to cool temperature. This call reactivity deficit is
433 specific to cool exposure and is not the result of an acute dam separation. Moreover, we
434 demonstrate that the oxytocinergic system modulates this neonatal thermosensibility.
435 By exploring possibilities of peripheral and central origins of this deficit, we found BAT
436 activation upon cool challenge, suggesting that the autonomic neural circuit including
437 expression of thermoreceptors of dorsal root ganglion controlling non-shivering thermogenesis
438 is not affected. Furthermore, functional investigation of the Grueneberg ganglion, a
439 thermosensory system present at the tip of the nose, revealed that this peripheral cool sensor
440 is still active in *Magel2*$^{+/-p}$ neonates. However, we cannot completely exclude a peripheral
441 deficit through a dysfunction of the trigeminal ganglion since it contains thermosensory
442 neurons detecting orofacial cool stimuli and it expresses Magel2 (*49, 50*). The nasal branch of
443 the trigeminal nerve also expresses OT receptors that can be activated after IN administration
444 of OT (*51-53*).
445 *Magel2*$^{+/-p}$ neonates might encounter not only difficulties in detecting but also in integrating
446 thermo-sensory stimuli. Here, we provided some evidences for the hypothesis of a central
447 origin. First, we found a lack of cool-induced alteration of brain pERK signaling and second,
448 we showed that brain inactivation of OT neurons in WT reproduces atypical thermo-sensory
449 reactivity.
450 We have provided previous evidences that the oxytocinergic system is altered in *Magel2*$^{+/-p}$
451 mice and that early OT treatment restores normal motor sucking activity, social and cognitive
452 behaviors in adult mice (*31, 32*). Furthermore clinical trials conducted previously in Prader-
453 Willi babies have demonstrated the efficiency of intranasal oxytocin administration to rescue
454 sucking activity (*54*). Prader-Willi and Schaaf-Yang babies present also sensory disorders
455 characterized in particular by temperature instabilities manifested by episodes of hyper or

456 hypothermia without infectious causes (*26, 27*). Moreover, adolescent with ASD present loss
457 of sensory function for thermal perception (28). Here we demonstrate a new pivotal role of the
458 oxytocinergic system in modulating early life thermosensory function that could be involved in
459 these symptoms.

460 Although cool-induced cry has been also observed in newborn infants more than 20 years ago
461 (*55*), it is rarely observed nowadays because maintaining the body temperature of the neonate
462 has been emphasized. Measures of early life sensory behavior such as cool-thermosensory
463 call behavior might represent promising avenues for early diagnostic and OT treatment could
464 be considered for therapeutic interventions of this atypical sensory reactivity.

465

466 **MATERIAL AND METHODS**

467 **Animals**

468 Mice were handled and cared in accordance with the Guide for the Care and Use of Laboratory
469 Animals (N.R.C., 1996) and the European Communities Council Directive of September 22th,
470 2010 (2010/63/EU, 74). Experimental protocols were approved by the institutional Ethical
471 Committee Guidelines for animal research with the accreditation no. B13-055-19 from the
472 French Ministry of Agriculture. All efforts were made to minimize the number of animals used.
473 129-Gt(ROSA)26Sor$^{tm1(CAG-CHRM4*,-mCitrine)Ute}$ also known as R26-LSL-hM4Di DREADD were
474 obtained from the Jackson Laboratory (stock #026219) and called here hM4Di DREADD mice
475 for convenience. Due to the parental imprinting of *Magel2* only heterozygous mice (+m/-p) with
476 the mutated allele transferred by the male were used for experiments. The OT-cre mice were
477 obtained from the Jackson Laboratory (stock #24234). In our experiment we used hM4Di
478 DREADD homozygous // heterozygous OT-cre mice (referred here as OT hm4DI).

479

480 **USV recording**

481 On the day of testing (P0, P1, P2, P3 and P6), each pup was separated from its littermates
482 and dam after 30 min of habituation to the testing room, placed on a heating pad and each pup
483 were isolated in a box (23 × 28 × 18 cm) located inside an anechoic box (54 × 57 × 41 cm;
484 Couldbourn instruments, PA, USA) for a 5 min test at room temperature (25°C). Then the pup
485 goes back to the dam for 5-10 min and submits a second separation, placed on a heating pad
486 and the USV were recorded during 5 min under cool temperature (17°C). An ultrasound
487 microphone (Avisoft UltraSoundGate condenser microphone capsule CM16/CMPA, Avisoft
488 bioacoustics, Germany) sensitive to frequencies of 10–250 kHz was located in the roof of the
489 isolation box. Recordings were done using Avisoft recorder software (version 4.2) with a
490 sampling rate of 250 kHz in 16 bits format. Data were transferred to SASLab Pro software
491 (version 5.2; Avisoft bioacoustics) and a fast Fourier transformation was conducted (256 FFT-
492 length, 100% frame, Hamming window, and 75%-time window overlap) before the analysis.
493 Recordings were analyzed for the number of calls during the 5 min recording at 25°C and 17°C
494 and for the latency which is the first ultrasound call of the record. The cooling responsive rate
495 was calculated as the proportion of pups responsive to cooling: a pup is responsive if the
496 latency is two time shorter at 17°C than 25°C.

497

498 **Animals' treatment**

499 The solutions injected were isotonic saline (10 µl) for the control mice and 2 µg of OT (Phoenix
500 Pharmaceuticals Inc., cat #051-01) or 0.2 µg (Thr^4,Gly^7)-Oxytocin(TGOT) (BACHEM, lot
501 #1062174) or 0.25 µg of Vasopressin (Phoenix Pharmaceuticals Inc., cat #065-07) diluted in
502 isotonic saline (10 µl) for the treated mice. Intranasal administration was performed in P2
503 mice 10 min before USV recording.

504 CNO (Clozapine-N-oxide; Sigma-Aldrich, St Louis, MO, USA) was dissolved in dimethyl
505 sulfoxide (DMSO; Sigma-Aldrich, St Louis, MO, USA) and diluted with 0.9% isotonic saline
506 to volume, the DMSO concentrations in the final CNO solutions were 0.5%. 1µg of CNO

507 was administrated by subcutaneous route in a total volume of 10µl. Administration was
508 performed in P2 mice 2 h-2 h30 before USV recording.

509 **Corticosterone immunoassay**

510 P2 mice were separated from their mother and placed on a heating pad for 5 min., then
511 sacrificed and blood samples were quickly collected. Blood serum was separated by
512 centrifugation (5,000 rpm, 20 min) and stored at -80°C. Serum corticosterone concentrations
513 were measured with corticosterone ELISA kit (Enzo Life Sciences, Farmingdale, NY, USA)
514 according to the manufacturer's instructions.

515 ***Lipids analysis***

516 BATs from P2 pups were extracted and incubated with 500 µL of Chloroform/Methanol
517 ($CHCl_3$:CH_3OH, 2:1 *v/v*) solution. Organic phase was isolated by centrifugation at
518 10,000 rpm, washed by 0.2 vol of 0.9% NaCl solution, dried over $MgSO_4$ and then
519 concentrated under nitrogen stream.
520 19 µL of CH_2Cl_2 were added per mg of BAT. For TAG analysis, 2 µL of extract
521 containing total lipids were separated on TLC (Silica Gel 60, Merck) by using petroleum
522 ether:diethyl ether (90:10, *v*/*v*) as eluent. For DAG, MAG and FA analysis, 5 µL of the
523 same samples were separated on TLC by using heptane:diethyl ether:formic acid
524 (55:45:1, v/v/v) as eluent. The TLC plates were sprayed with a solution of 5%
525 phosphomolybdic acid in ethanol followed by heating at 120°C in an oven for 5-10 min,
526 to visualize the spots.
527 Each resolved plate was scanned using a Chemidoc™ MP Imaging System (Bio-Rad),
528 and densitometric analyses were performed using the ImageLab™ software version
529 5.0 (Bio-Rad) to determine relative TAG content per sample.

530 **Calcium imaging**

531 Grueneberg ganglion slices (400µm) were incubated with 10 µM of Fura-2-AM (Life
532 technologies) added with Pluronic acid and dissolved in DMSO, for 45 min at 33°C in an
533 oxygenated artificial cerebrospinal fluid (aCSF) dark chamber. aCSF composition was as
534 followed (in mM): 126 NaCl, 3.5 KCl, 2 $CaCl_2$, 1.3 $MgCl_2$, 1.2 NaH_2PO_4, 25 $NaHCO_3$ and 11
535 glucose, pH 7.4 equilibrated with 95% O_2 and 5% CO_2. The recording chamber was first filled
536 with warm (30°C) aCSF for 1 min, then perfused with cool (15°C) aCSF for 3 min and then
537 warm with aCSF for 1 min. Images were acquired every 5 sec with an Olympus BX61WI
538 microscope equipped with a multibeam multiphoton pulsed laser scanning system (LaVision
539 BioTecs) as previously described (Crépel et al., 2007). Images were acquired through a CCD
540 camera, which typically resulted in a time resolution of 50–150 ms per frame. Slices were
541 imaged using a 20×, NA 0.95 objective (Olympus). Images were collected by CCD-based
542 imaging system running ImspectorPro software (LaVision Biotec) and analyzed with Fiji
543 software (*56*).

544 **Protein extraction and Western blotting**

545 Brain and brown adipose tissues were homogenized in RIPA buffer (Thermo Fisher Scientific)
546 with phosphatase and protease inhibitor cocktails (Pierce Protease and Phosphatase Inhibitor
547 Mini Tablets, EDTA-Free) added with 1% Triton (Euromedex, life sciences products) for the
548 brown adipose tissues. Proteins were run on polyacrylamide gel (Bolt 4-12% Bis Tris plus,
549 Invitrogen by Thermo Fisher Scientific) and transferred to a nitrocellulose membrane (GE
550 Healthcare Life Science). Primary antibodies were incubated overnight at 4°C and were as
551 follow: UCP1 (1:1000, Cell Signalling technology, #14670); p44/42 MAPK (1:1000, Cell
552 Signalling technology, #9102); phospho-p44/42 MAPK (1:1000, Cell Signalling technology,
553 #9101); GAPDH (1:1000, Invitrogen#PA1987). Signals were detected using Super Signal West
554 Pico (Thermo Fisher Scientific, #34080) and bands were analyzed with ImageJ.

555 **Reverse transcription and real time quantitative PCR**

556 Wild-type and mutant newborns were sacrificed at P2 (between 2pm and 4pm). The
557 hypothalamus, BAT and dorsal root ganglia tissues were quickly dissected on ice and rapidly
558 frozen in liquid nitrogen, then stored at -80°C. Total RNA was isolated using the RNeasy® Mini
559 Kit (Qiagen, cat #74104), according to the manufacturer's protocol and cDNAs were obtained
560 by reverse transcription using QuantiTect® Reverse Transcription Kit (Qiagen, cat #205311),
561 starting with 600 ng of total RNA.
562

563 **Temperature**

564 The body surface temperature was measured using an infrared medical thermometer.
565 Temperature's values were taken every 30 sec during 5 min at room temperature (25°C) and
566 every 30 sec during 5 min at 17°C.

567

568 **Statistical analysis**

569 Analyses were performed using non-parametric statistical tools when the size of the samples
570 was small (GraphPad, Prism 6 software) and the level of significance was set at P<0,05.
571 Values are indicated as following: (Q2 (Q1, Q3) or mean±SEM, n, p-value, statistical test)
572 where Q2 is the median, Q1 is the first quartile and Q3 is the third quartile. Appropriate tests
573 were conducted depending on the experiment and are indicated in the figure legends. Mann-
574 Whitney (MW) test was run to compare two unmatched groups and Wilcoxon- Mann-Whitney
575 (WMW) to compare two matched groups. Kruskal-Wallis (KW) followed by a post hoc test Dunn
576 test was run to compare three or more independent groups. Fisher's exact test was run to
577 compare contingency tables (reactive vs unreactive animals to cool exposure). Two-way
578 ANOVA followed by Bonferroni post-hoc test was performed to compare the effect of two
579 factors on unmatched groups.
580

ACKNOWLEDGMENTS

We thank Antonin Vinck and Emmanuelle Brot for their technical help and the members of the animal facility, genotyping and imaging platforms of INMED laboratory. We thank Dr N. Kourdougli, Pr C. Rivera and C Pellegrino for comments. This study has been supported by INSERM, Aix-Marseille Univ., Foundation Lejeune (N°R15117AA) and ANR (PRADOX N°14-CE13-0025), 20 and Prader Willi France foundation grants. L.C was supported by a PhD fellowship from the French Minister for Research and Technology and from the support of A*MIDEX/ANR (Neuro*AMU Neuroschool PhD program) funded by the French Government « Investissements d'Avenir » program. The authors declare no competing financial interests.

REFERENCES

1. C. E. Robertson, S. Baron-Cohen, Sensory perception in autism. *Nature Reviews Neuroscience* **18**, 671-684 (2017).
2. G. T. Baranek *et al.*, Hyporesponsiveness to social and nonsocial sensory stimuli in children with autism, children with developmental delays, and typically developing children. *Dev. Psychopathol.* **25**, 307-320 (2013).
3. A. Estes *et al.*, Behavioral, cognitive, and adaptive development in infants with autism spectrum disorder in the first 2 years of life. *Journal of Neurodevelopmental Disorders* **7**, 24 (2015).
4. L. L. Orefice *et al.*, *Cell* **166**, 299-313 (2016).
5. G. Chelini *et al.*, Aberrant Somatosensory Processing and Connectivity in Mice Lacking Engrailed-2. *J Neurosci* **39**, 1525-1538 (2019).
6. T. N. Huang *et al.*, Haploinsufficiency of autism causative gene Tbr1 impairs olfactory discrimination and neuronal activation of the olfactory system in mice. *Mol Autism* **10**, 5 (2019).
7. J. K. Siemann *et al.*, An autism-associated serotonin transporter variant disrupts multisensory processing. *Transl Psychiatry* **7**, e1067 (2017).
8. N. Cheng, M. Khanbabaei, K. Murari, J. M. Rho, Disruption of visual circuit formation and refinement in a mouse model of autism. *Autism Res* **10**, 212-223 (2017).
9. E. Drapeau, M. Riad, Y. Kajiwara, J. D. Buxbaum, Behavioral Phenotyping of an Improved Mouse Model of Phelan-McDermid Syndrome with a Complete Deletion of the Shank3 Gene. *eNeuro* **5**, (2018).
10. C. X. He *et al.*, Tactile Defensiveness and Impaired Adaptation of Neuronal Activity in the Fmr1 Knock-Out Mouse Model of Autism. *J Neurosci* **37**, 6475-6487 (2017).

617 11. L. Balasco, G. Provenzano, Y. Bozzi, Sensory Abnormalities in Autism Spectrum Disorders: A
618 Focus on the Tactile Domain, From Genetic Mouse Models to the Clinic. *Front Psychiatry* **10**,
619 1016 (2019).
620 12. S. K. Wixson, K. L. Smiler, in *Anesthesia and Analgesia in Laboratory Animals*. (Elsevier, 1997),
621 pp. 165-203.
622 13. G. L. Oswalt, G. W. Meier, Olfactory, thermal, and tactual influences on infantile ultrasonic
623 vocalization in rats. *Dev Psychobiol* **8**, 129-135 (1975).
624 14. M. S. Blumberg, I. V. Efimova, J. R. Alberts, Ultrasonic vocalizations by rat pups: the primary
625 importance of ambient temperature and the thermal significance of contact comfort. *Dev*
626 *Psychobiol* **25**, 229-250 (1992).
627 15. H. Szentgyörgyi, J. Kapusta, A. Marchlewska-Koj, Ultrasonic calls of bank vole pups isolated and
628 exposed to cold or to nest odor. *Physiology & Behavior* **93**, 296-303 (2008).
629 16. R. Bumbalo *et al.*, Grueneberg Glomeruli in the Olfactory Bulb are Activated by Odorants and
630 Cool Temperature. *Cell. Mol. Neurobiol.* **37**, 729-742 (2017).
631 17. Y. C. Chao *et al.*, Receptor guanylyl cyclase-G is a novel thermosensory protein activated by
632 cool temperatures. *The EMBO Journal* **34**, 294-306 (2015).
633 18. K. Mamasuew, H. Breer, J. Fleischer, Grueneberg ganglion neurons respond to cool ambient
634 temperatures. *Eur. J. Neurosci.* **28**, 1775-1785 (2008).
635 19. K. Mamasuew *et al.*, Chemo- and thermosensory responsiveness of Grueneberg ganglion
636 neurons relies on cyclic guanosine monophosphate signaling elements. *Neurosignals* **19**, 198-
637 209 (2011).
638 20. J. Fleischer, H. Breer, The Grueneberg ganglion: a novel sensory system in the nose. *Histol.*
639 *Histopathol.* **25**, 909-915 (2010).
640 21. H. Hashimoto, N. Moritani, S. Aoki-Komori, M. Tanaka, T. R. Saito, Comparison of ultrasonic
641 vocalizations emitted by rodent pups. *Exp. Anim.* **53**, 409-416 (2004).
642 22. M. E. Symonds, M. Pope, H. Budge, The Ontogeny of Brown Adipose Tissue. *Annual Review of*
643 *Nutrition* **35**, 295-320 (2015).
644 23. R. Oelkrug, E. T. Polymeropoulos, M. Jastroch, Brown adipose tissue: physiological function
645 and evolutionary significance. *Journal of Comparative Physiology B* **185**, 587-606 (2015).
646 24. I. Boccaccio *et al.*, The human MAGEL2 gene and its mouse homologue are paternally
647 expressed and mapped to the Prader-Willi region. *Hum. Mol. Genet.* **8**, 2497-2505 (1999).
648 25. C. P. Schaaf *et al.*, Truncating mutations of MAGEL2 cause Prader-Willi phenotypes and autism.
649 *Nature Genetics* **45**, 1405-1408 (2013).
650 26. S. B. Cassidy, S. Schwartz, J. L. Miller, D. J. Driscoll, Prader-Willi syndrome. *Genetics in Medicine*
651 **14**, 10-26 (2012).
652 27. J. McCarthy *et al.*, Schaaf-Yang syndrome overview: Report of 78 individuals. *Am. J. Med.*
653 *Genet. A* **176**, 2564-2574 (2018).
654 28. E. G. Duerden *et al.*, Decreased Sensitivity to Thermal Stimuli in Adolescents With Autism
655 Spectrum Disorder: Relation to Symptomatology and Cognitive Ability. *The Journal of Pain* **16**,
656 463-471 (2015).
657 29. V. Grinevich, R. Stoop, Interplay between Oxytocin and Sensory Systems in the Orchestration
658 of Socio-Emotional Behaviors. *Neuron* **99**, 887-904 (2018).
659 30. C. Harshaw, J. K. Leffel, J. R. Alberts, Oxytocin and the warm outer glow: Thermoregulatory
660 deficits cause huddling abnormalities in oxytocin-deficient mouse pups. *Hormones and*
661 *Behavior* **98**, 145-158 (2018).
662 31. H. Meziane *et al.*, An Early Postnatal Oxytocin Treatment Prevents Social and Learning Deficits
663 in Adult Mice Deficient for Magel2, a Gene Involved in Prader-Willi Syndrome and Autism.
664 *Biological Psychiatry* **78**, 85-94 (2015).
665 32. F. Schaller *et al.*, A single postnatal injection of oxytocin rescues the lethal feeding behaviour
666 in mouse newborns deficient for the imprinted Magel2 gene. *Hum. Mol. Genet.* **19**, 4895-4905
667 (2010).

33. P. Kromkhun *et al.*, Quantitative and qualitative analysis of rat pup ultrasonic vocalization sounds induced by a hypothermic stimulus. *Lab Anim Res* **29**, 77-83 (2013).
34. J. T. Allin, E. M. Banks, Effects of temperature on ultrasound production by infant albino rats. *Dev Psychobiol* **4**, 149-156 (1971).
35. T. Yahiro, N. Kataoka, Y. Nakamura, K. Nakamura, The lateral parabrachial nucleus, but not the thalamus, mediates thermosensory pathways for behavioural thermoregulation. *Scientific Reports* **7**, (2017).
36. S. V. Kozlov *et al.*, *Nature Genetics* **39**, 1266-1272 (2007).
37. V. Matarazzo, F. Muscatelli, Natural breaking of the maternal silence at the mouse and human imprinted Prader-Willi locus: A whisper with functional consequences. *Rare Dis* **1**, e27228 (2013).
38. K. Townsend, Y.-H. Tseng, Brown adipose tissue: Recent insights into development, metabolic function and therapeutic potential. *Adipocyte* **1**, 13-24 (2012).
39. F. Muscatelli, M. G. Desarménien, V. Matarazzo, V. Grinevich, in *Behavioral Pharmacology of Neuropeptides: Oxytocin,* R. Hurlemann, V. Grinevich, Eds. (Springer International Publishing, Cham, 2017), vol. 35, pp. 239-268.
40. H. Zhu *et al.*, Cre-dependent DREADD (Designer Receptors Exclusively Activated by Designer Drugs) mice. *Genesis* **54**, 439-446 (2016).
41. M. Jendryka *et al.*, Pharmacokinetic and pharmacodynamic actions of clozapine-N-oxide, clozapine, and compound 21 in DREADD-based chemogenetics in mice. *Scientific Reports* **9**, 4522 (2019).
42. A.-K. Ilg, T. Enkel, D. Bartsch, F. Bähner, Behavioral Effects of Acute Systemic Low-Dose Clozapine in Wild-Type Rats: Implications for the Use of DREADDs in Behavioral Neuroscience. *Frontiers in Behavioral Neuroscience* **12**, (2018).
43. M. R. Lee *et al.*, Oxytocin by intranasal and intravenous routes reaches the cerebrospinal fluid in rhesus macaques: determination using a novel oxytocin assay. *Molecular Psychiatry* **23**, 115-122 (2018).
44. D. S. Quintana *et al.*, Advances in the field of intranasal oxytocin research: lessons learned and future directions for clinical research. *Mol Psychiatry*, (2020).
45. M. Wallis, Molecular evolution of the neurohypophysial hormone precursors in mammals: Comparative genomics reveals novel mammalian oxytocin and vasopressin analogues. *Gen. Comp. Endocrinol.* **179**, 313-318 (2012).
46. M. Manning *et al.*, Oxytocin and Vasopressin Agonists and Antagonists as Research Tools and Potential Therapeutics: Oxytocin and vasopressin agonists and antagonists. *Journal of Neuroendocrinology* **24**, 609-628 (2012).
47. S.-Y. Lee *et al.*, Oxytocin Protects Hippocampal Memory and Plasticity from Uncontrollable Stress. *Scientific Reports* **5**, (2016).
48. R. A. Whittington *et al.*, Anesthesia-induced hypothermia mediates decreased ARC gene and protein expression through ERK/MAPK inactivation. *Scientific Reports* **3**, 1388 (2013).
49. S. F. Morrison, K. Nakamura, Central Mechanisms for Thermoregulation. *Annual Review of Physiology* **81**, 285-308 (2019).
50. R. Vaidyanathan, F. Schaller, F. Muscatelli, E. A. D. Hammock, Colocalization of Oxtr with Prader-Willi syndrome transcripts in the trigeminal ganglion of neonatal mice. *Hum Mol Genet* **29**, 2065-2075 (2020).
51. Y. Murata, M.-Z. Li, S. Masuko, Developmental expression of oxytocin receptors in the neonatal medulla oblongata and pons. *Neuroscience Letters* **502**, 157-161 (2011).
52. D. S. Quintana, K. T. Smerud, O. A. Andreassen, P. G. Djupesland, Evidence for intranasal oxytocin delivery to the brain: recent advances and future perspectives. *Therapeutic Delivery* **9**, 515-525 (2018).
53. A. Tzabazis *et al.*, Oxytocin receptor: Expression in the trigeminal nociceptive system and potential role in the treatment of headache disorders. *Cephalalgia* **36**, 943-950 (2016).

54. M. Tauber *et al.*, The Use of Oxytocin to Improve Feeding and Social Skills in Infants With Prader–Willi Syndrome. *Pediatrics* **139**, e20162976 (2017).
55. B. Petrikovsky, M. Silverstein, E. P. Schneider, Neonatal shivering and hypothermia after intrapartum amnioinfusion. *The Lancet* **350**, 1366-1367 (1997).
56. J. Schindelin *et al.*, Fiji: an open-source platform for biological-image analysis. *Nat. Methods* **9**, 676-682 (2012).